

1

Mechanical Properties of Nanocrystalline Materials

Pasquale Cavaliere

1.1

Introduction

Nanostructured materials attracted a wide scientific interest in the past decade. The strength of metals and alloys is strongly influenced by the grain size. The attractive properties of nanocrystalline (NC) metals and alloys are the high yield and fracture strength, the improved wear resistance, and the superplastic behavior at relatively low temperatures and high strain rates as compared to microcrystalline (MC) materials. NC metals also exhibit high strain rate sensitivity as compared to MC materials [1, 2]. The strength of the metals is related to the microstructure as described by the well-known Hall–Petch (H-P) relationship. Generally, it is observed that the rate of strength increases by decreasing the mean grain size below 100 nm and the strength decreases by decreasing the grain size below about 20–10 nm mean grain size; such a behavior has been commonly indicated as H-P breakdown, implying a transition in the deformation modes of metals by decreasing the grain size from NC range down to very low levels. Recent investigation has suggested that dislocation-accommodated boundary sliding is the main deformation process governing the entire deformation in NC metals [3]. Actually, different processing methods are available to produce ultrafine-grained materials (UFG), such as mechanical alloying (at room and low temperatures) with consequent consolidation (compaction and/or extrusion) and severe plastic deformation (SPD) (high-pressure torsion [4], HPT or equal-channel angular pressing [5], ECAP), generally leading to the production of UFG materials [6, 7] and gas-phase condensation of particles with consequent consolidation or electrodeposition capable of producing metals in the range of NC grain size. SPD is useful in producing bulk materials with enhanced strength, hardness, and wear and superplastic properties at relatively a low temperature and high strain rates. Some of the general properties in the available literature are summarized in Table 1.1. The mechanisms of deformation and the properties of the material not only depend on the average grain size but are also strongly influenced by the grain size distribution and grain boundary structure (e.g., low-angle versus high-angle grain boundaries). The wide application of UFG NC metals in the modern industry is related

Table 1.1 Properties of ultrafine and NC materials produced via different techniques.

Material	Processing method	Grain size (nm)	Hardness	Yield strength (MPa)
Pure Ni	HPT	170–900	3.5–1.5 GPa	1100–700
Pure Ti	HPT	80–300	315–240 Hv	960–730
Ti–6Al–4V	HPT	100–300	400–320 Hv	1300–1080
Pure Al	ECAP	600–900	60–45 Hv	140–90
Al–Mg–Sc	ECAP	200–400	100–80 Hv	580–420
Pure Ni	ED	10–200	7.5–3.5 GPa	1600–800
Ni–W	ED	7–90	8–6 GPa	1800–1000

to the increased understanding of their damage resistance and of the mechanical mechanisms involved in the deformation, particularly under cyclic loading. As a general behavior, it was observed that the fatigue limit of NC metals increases with decreasing grain size, and the crack initiation susceptibility decreases with increasing crack growth rate coupled with grain refinement [8]. The main damage mechanism has been recognized in the early strain localization and micro-crack formation for ECAP materials. In general, a high decrease in the fatigue properties was shown for SPD materials in the low cycle fatigue (LCF) regime of intermediate-to-high plastic strain amplitudes. On the contrary, in the high cycle fatigue (HCF) regime of intermediate-to-low plastic strain amplitudes, it results in high enhancement of the fatigue resistance for materials with grain refinement. In MC materials, a reduction in the grain size generally results in an increase in strength, which engenders an increase in the fatigue endurance limit during stress-controlled cyclic loading of initially smooth-surfaced laboratory specimens.

As the total fatigue life under the aforementioned conditions is dominated by crack nucleation and as the fatigue cracks generally nucleate at the free surface, grain refinement is considered to result in improvements in fatigue life and endurance limit, with all other structural factors set aside. On the other hand, a coarse grain structure with lower strength and enhanced ductility generally plays a more beneficial role in the strain-controlled fatigue response of metals and alloys. It should be noted, however, that it is often difficult to isolate the sole effects of grain size on fatigue response because other structural factors such as precipitate content, size and spatial distribution, stacking fault energy and the attendant equilibrium spacing of partial dislocations, and crystallographic texture are also known to have an important effect on the fatigue characteristics of MC metals. In NC materials with finest grains, plastic flow is conducted mostly by grain boundary processes. In NC materials with intermediate grains, plastic flow is often conducted by both lattice dislocation slip and grain boundary processes. However, if plastic flow and diffusion are not intensive in NC materials with intermediate grains, and/or these materials contain pre-existent nanocracks and pores, brittle fracture tends to occur. Dimpled rupture, dislocation activity at the crack tip, and formation of voids at grain boundaries and triple junctions in the regions ahead of the advancing crack were observed. In the early stages

of deformation, dislocations are emitted from the grain boundaries under the influence of the applied stress. Triple junction voids and wedge cracks can also result from grain boundary sliding if the resulting displacements at the boundary are not accommodated by diffusional or power-law creep. These grain boundary and triple junction voids then act as sites for nucleation of the dimples. The deformation and fracture processes are closely related to the coupling of dislocation-mediated plasticity and formation and growth of voids. Irrespective of the fracture mechanism, it is evident that the fracture is heavily influenced by the microstructural features such as the presence of nanoscale voids or bubbles and the presence of grown-in twins, which have, so far, been mostly neglected [9]. The presence of grown-in twins has been suggested as an interface control mechanism in coarse-grained metals, and they represent a relevant microstructural feature that influences fracture, as many of the NC metals contain grown-in twins. The aim of this chapter is to provide a deep and complete understanding on the overall microstructural and mechanical properties of nanostructured metals and alloys.

1.2

Static Properties

1.2.1

Tensile Behavior

The strength of metals is related to the microstructure as described by the well-known H-P relationship. Generally, it is observed that the rate of strength increases by decreasing the mean grain size below 100 nm, and the strength decreases by decreasing the grain size below about 20–10 nm mean grain size; such a behavior has been commonly indicated as H-P breakdown, implying a transition in the deformation modes of metals by decreasing the grain size from NC range down to very low levels. In these alloys produced via SPD, which leads to materials characterized by ultrafine grains, the yield and ultimate tensile strengths increase with decreasing grain size; such an increase in yield is generally related to the deformation level such as the number of passes in ECAP (Figure 1.1), and such an increase in strength is generally coupled with a decrease in the material ductility [10].

As clearly shown in Figure 1.2, aluminum alloys subjected to SPD via ECAP exhibit a different strain softening as a function of the number of passes. The stability of the mechanical properties is governed by precipitation, and in the alloys strengthened by stable precipitates inhibiting grain growth by impeding grain boundary mobility, the materials exhibit finer structures at the same level of SPD. An interesting example is shown for AA6XXX reinforced with Sc–Zr and produced via ECAP (Figure 1.2). After SPD and aging, the 6106 Sc alloy is stronger than the 6106 Zr alloy under the same condition, because of the

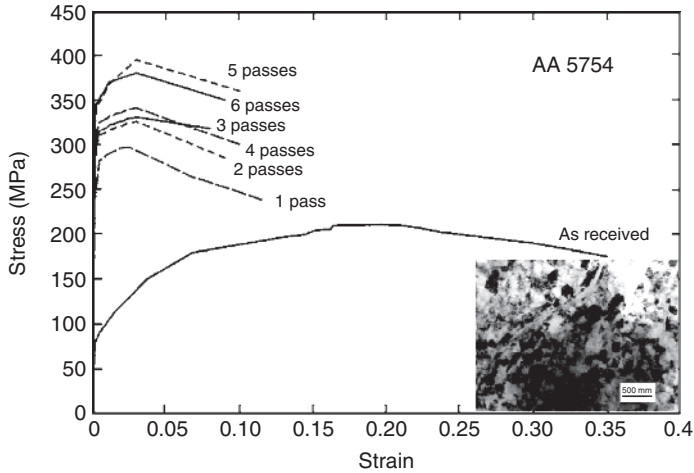


Figure 1.1 Stress versus strain at room temperature when testing under tension at an initial strain rate of $3 \times 10^{-3} \text{ s}^{-1}$; curves are shown for the as-received AA5754 and after pressing through one to six passes.

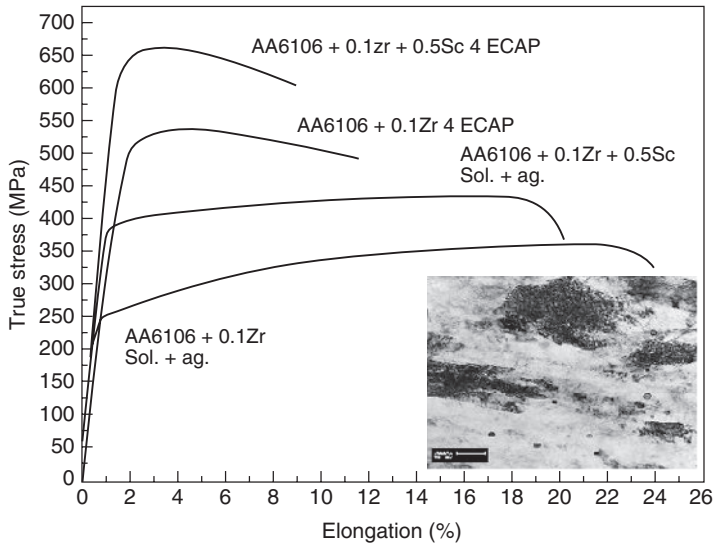


Figure 1.2 Tensile response of the 6106 Zr and 6106 Sc alloys after solution treatment + ageing, and solution treatment + ECAP + ageing conditions.

more effective precipitation hardening in the Sc–Zr-modified alloy [11]. The $\text{Al}_3(\text{Zr}_{1-x}\text{Sc}_x)$ precipitates have been demonstrated to provide more effective hardening and are more stable at high temperatures as compared to Al_3Zr . In addition, the effectiveness of the different particles on grain refinement is

stronger in the case of Sc-modified alloys (170 μm after four passes) as compared to the Zr-modified alloy (200 μm after four passes).

As in the case of 5754 alloy, after ECAP, the alloys exhibit strain softening leading to failure after reaching the maximum tensile peak. Such a behavior is normally observed in very complex alloys, whereas it is not observed in pure metals such as Ni produced via electrodeposition (Figure 1.3a), and it can also be explained in terms of dislocation generation and rearrangement. It is clear that this phenomenon is much more pronounced in the materials obtained through SPD. In fact, also in the case of Ni–W alloys produced via electrodeposition (Figure 1.3b), we can underline the absence of softening with strain, demonstrating that such a behavior is related to the dislocation density and energy being much higher than those in the materials produced via SPD.

It should be underlined that the very low level of macroscopic tensile ductility in NC fcc metals is due to the localization of deformation demonstrated by the observation of the fracture surface in the tensile tested specimens. In such materials, in fact, the fracture surfaces comprise dimples larger than the original grain size, and the number of dimples increases with decreasing material grain size. In general, while electrodeposited NC Ni and Ni–W alloys exhibit deformation behavior with decrease in grain refinement down to a quasi-absence due to reduction in the fractured area, in UFC materials, a detectable necking is observed. For electrodeposited NC metals, the strength increases with decreasing grain size. Strain softening is not observed in these metals, owing to the lower energy of dislocations with respect to severely deformed materials such as those produced via ECAP. Recovery is not observed in deformed NC metals. On the contrary, room temperature recovery can be demonstrated in ultrafine materials produced via ECAP or HPT. The deformation mechanism, ductility, hardening–softening behavior, and strain rate sensitivity are strongly related to one another. These features are discussed in the next section.

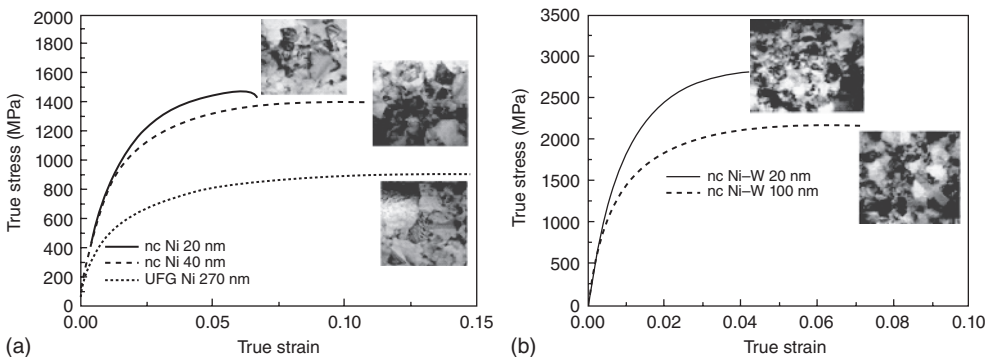


Figure 1.3 Tensile behavior of pure Ni with a different grain size produced via electrodeposition (a), Ni–W alloy with a different grain size (b).

1.2.2

Nanoindentation

With the development of nanostructured metals and alloys, instrumented nanoindentation seems to be very useful in obtaining the fundamental mechanical properties and for understanding the fundamental material physics. This characterization technique is a very powerful tool, because of the fact that the tested volume of material is compatible with the microstructure. Many papers were presented in the literature on nanostructured material characterization through instrumented nanoindentation; in addition to hardness and yield strength (Figure 1.4), such a characterization technique seems to be very useful in the analyses of material hardening and/or softening [12].

This technique has also been employed to provide experimental evidence of the dynamic properties of NC materials. Nanoindentation fatigue experiments can provide very useful information on plastic zone propagation, cyclic hardening, and crack nucleation and growth in nanostructured materials. The material behavior can be explained similarly to crack propagation. In static loading, the plasticity surrounding the crack tip either blunts the crack or shields the crack tip from the external stress. Dynamic loading leads to a dynamic process between the effective applied stress and the internal stress, which is similar to the dislocation generation and annihilation to the crack tip in the conventional crack propagation tests [13]. Multistep nanoindentation is an interesting technique. A fixed strain (in terms of indentation depth) is reached in a single indentation or through increasing levels of deformation, indicating a variation in the mechanical properties of the material by a difference in the hardness values implying the hardening or softening behavior of the tested material (Figure 1.5). Another fundamental aspect is represented by the possibility of calculating the material strain rate sensitivity through

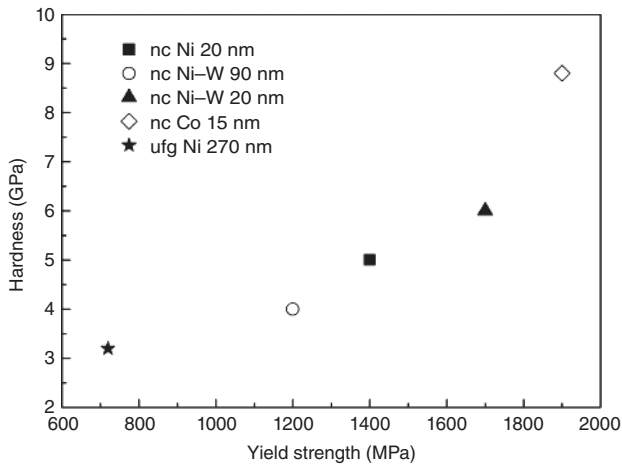


Figure 1.4 Hardness and yield strength measure obtained by instrumented nanoindentation for different nanostructured materials.

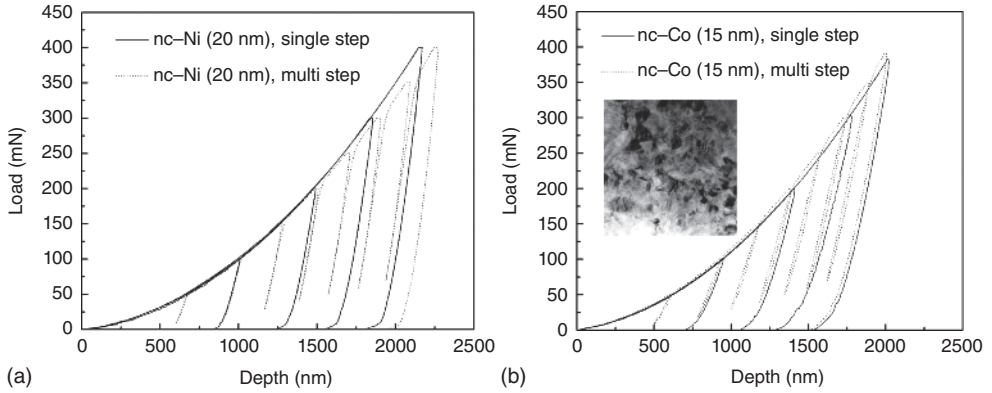


Figure 1.5 Nanoindentation behavior for pure electrodeposited Ni showing hardening (a), for pure electrodeposited Co showing softening (b).

the loading rate variation during nanoindentation. High strain rate sensitivity can lead to a general improvement in the strength and ductility properties of the materials. A deeper understanding of this aspect can provide important information on the mechanical evolution of a large variety of NC metals for engineering applications.

The strain rate sensitivity of a material is defined as the variation in the flow stress with the strain rate at a given level of strain for a fixed temperature, and it can be expressed as:

$$m = \frac{\sqrt{3}kT}{\sigma v^*}$$

where k is the Boltzmann constant, T is the absolute temperature, σ is the flow stress, and v^* is the activation volume, which can be considered as the derivative of the activation energy with respect to the effective shear stress. By employing nanoindentation measurements, the flow stress can be related to the measured hardness ($H = 3\sigma$). The calculation of strain rate sensitivity is crucial in revealing many deformation mechanisms in nanostructured metals and alloys (Figure 1.6). Here, it is evident that a reduction in grain size from micro- to NC regime leads to an increase of an order of magnitude of strain rate sensitivity of plastic deformation. In general, the different behaviors observed for UFG and NC metals can be explained in terms of activation volume. A small activation volume of dislocation mobility is responsible for the variation in strain rate sensitivity with decreasing mean grain size of the metals. In addition, the mechanisms of dislocation generation at the grain boundaries coupled with grain rotation and migration are responsible for the entire plastic deformation in NC metals. Such mechanisms disappear by increasing the grain size from NC to UFG regime, thus decreasing the strain rate sensitivity of the materials at room temperature.

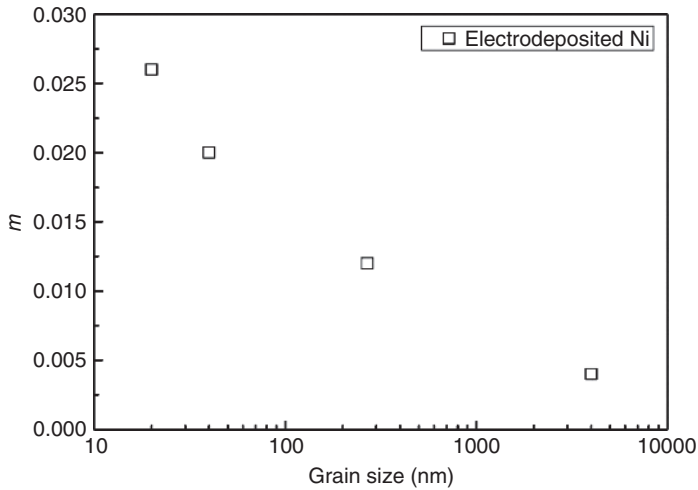


Figure 1.6 Room-temperature strain rate sensitivity of electrodeposited Ni with a different grain size.

1.3

Wear Properties

As in the case of tensile properties, wear behavior in metals is influenced by grain size [14]. The normal indentation test represents a limited application in predicting the tribological response. On the other hand, the scratch test, in which a hard indenter is slid across the surface of the material, is a tool for testing materials under conditions of controlled abrasive wear [15]. Frictional sliding or scratch testing is an alternative technique to characterize the hardness and response of materials in contact with hard indenters. During frictional sliding under conditions where the tip apex angle is sufficiently large to prevent the onset of discontinuous plasticity, a steady-state regime is reached after applying a constant normal force over a sufficient distance.

The characteristics of the residual scratch profile in this steady-state regime can be used to document the resistance and properties of the materials. From the scratch tests, it can be underlined that, with decreasing grain size, the material shows a significant increase in the friction coefficient (Table 1.2). Such a behavior becomes more evident by increasing the applied load and the penetration depth due to the different strain hardening of the material, which increases with decreasing mean grain size. In scratch tests, the normalized hardness and the normalized pile-up height are sufficient to determine the plastic strain hardening exponent and the initial yield strength. The friction coefficient decreases with increasing yield strength and strain hardening; however, the yield strength, due to grain refinement, appears more effective in improving the wear properties of the materials.

Table 1.2 Variation of friction coefficient with scratch load and penetration depth for electrodeposited nickel.

Material	Grain size (nm)	Penetration depth (nm)	Normal load (mN)	Friction coefficient
Pure NC Ni	20	5	0.2	0.35
Pure NC Ni	40	10	0.2	0.25
Pure UFG Ni	270	20	0.2	0.2
Pure NC Ni	20	35	0.5	0.53
Pure NC Ni	40	50	0.5	0.42
Pure UFG Ni	270	58	0.5	0.35
Pure NC Ni	20	80	1	0.65
Pure NC Ni	40	90	1	0.45
Pure UFG Ni	270	123	1	0.41

1.4
Fatigue Properties

The fatigue properties of materials are strongly governed by the grain size variation. Many experimental evidences can be presented both in the ultrafine and in the NC regime [16–18]. The first evidence can be underlined from the *S–N* curves of materials (Figure 1.7). In general, grain refinement via ECAP leads to an increase in fatigue properties in stress-controlled tests. The main damage mechanism has been recognized in the early strain localization and microcrack formation for the ECAP materials. In general, a strong decrease in fatigue properties was shown for SPD materials in the LCF regime of intermediate-to-high plastic strain amplitudes. On the contrary, in the HCF regime of intermediate-to-low plastic strain amplitudes, it results in high enhancement of the fatigue resistance for materials with grain refinement. In addition, it was observed that an annealing treatment, subsequent to the ECAP process, lead to enhancement of the LCF properties due

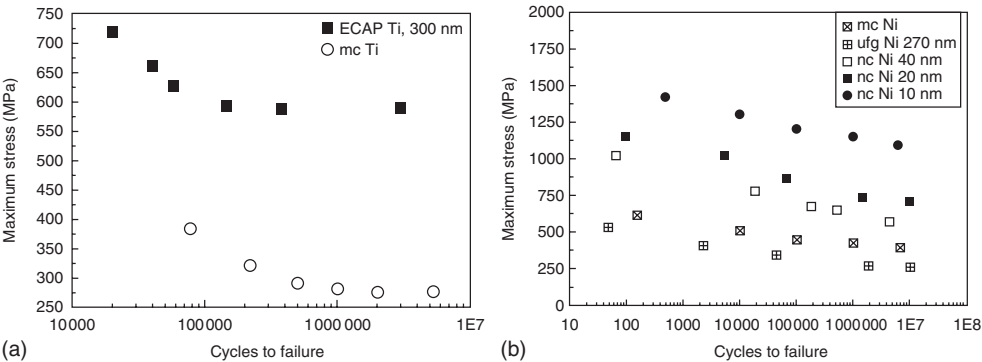


Figure 1.7 Fatigue curves of Ti produced via severe plastic deformation with UFC microstructure (a) and of Ni with ultrafine and NC microstructures (b).

to the increase in ductility. Such a behavior is obtained by partially recovering the grain boundary region that has been heavily distorted during processing. Pure UFG Ti, Al, and Ni show a decrease in ΔK threshold and an increase in crack propagation rate. On the contrary, pure Cu revealed higher susceptibility to crack initiation and a faster crack growth rate. Such a behavior is due to the different crack path related to the ductility variation after SPD demonstrated by the strain-controlled fatigue tests. For electrodeposited NC and UFG Ni, it was observed that the fatigue behavior of the materials is highly strain dependent. Even if grain refinement leads to an increase in the number of cycles to failure at the same stress levels investigated, the results for very close microstructures (20 and 40 nm) resulted in a strong function of the ductility (very high stresses).

In addition, by analyzing the strain amplitude as a function of the number of cycles to failure for all the electrodeposited materials, it can be concluded that the sensitivity to cyclic hardening increases by decreasing the material mean grain size.

1.5

Crack Behavior

Grain refinement, due to SPD, produces a decrease in ΔK threshold and an increase in crack propagation rate. The primary mechanism responsible for the accelerated fatigue crack growth rate observed with decreasing grain size is the reduction in crack path deflection with grain refinement. Microstructural size scales can play a dominant role in crack morphology and in the fracture mode, particularly near the threshold regime. Periodic deflections in the fatigue crack at the grain boundaries during crystallographic fracture can lead to a relatively tortuous crack path in coarser-grain materials. ECAP Ti exhibits a straight crack path, as compared to its MC counterpart (Figure 1.8a). The fatigue crack rate as a function of ΔK for all the Ni materials at a load ratio of $R = 0.25$ is shown in Figure 1.8b. At all the investigated stress levels, the material is less sensitive to crack initiation with decreasing mean grain size. On the other hand, the resistance to crack growth decreases with grain refinement. The fatigue crack rate as a function of ΔK for Co-based materials at a load ratio of $R = 0.25$ is shown in Figure 1.8c.

As a general trend, the crack growth rate is governed by the crack path. In the NC Co-based materials, the path appears very flat, and it is governed by the local brittleness of such NC metals, while in the case of MC materials, the path appears completely different with localized ductile. It was described that the possible intergranular fatigue crack growth behavior could be due to the high dislocation density in UFG materials, coupled with the presence of nonequilibrium grain boundaries due to trapping and accommodation of lattice dislocations during SPD. Small-sized grains lead to reduced flaw sizes and increased difficulties for the imposed stress concentration at the flaw to exceed the critical toughness of the material, thus suppressing early crack nucleation and propagation. In the grain size range of 100–500 nm, the deformation mechanisms are similar to those in

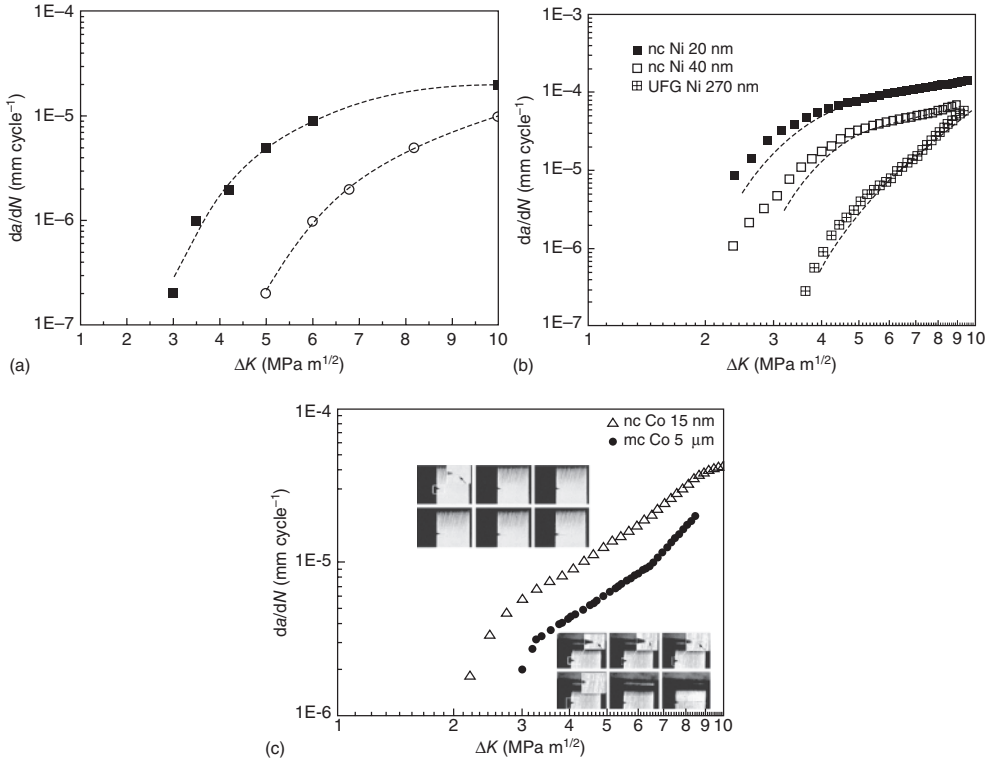


Figure 1.8 Crack growth behavior as a function of ΔK for the ECAP and MC pure Ti (a); crack growth rate as a function of ΔK for the electrodeposited pure Ni in the NC and UFG regimes (b); for NC Co as compared with its MC counterpart (c).

fine-grained traditional materials; whereas for grain sizes in the range of 50–100 nm, dislocations are emitted from, and are annihilated at, the grain boundaries; in the grain size range of 10–50 nm, partial dislocation emission and deformation twinning constitute the major deformation mechanisms; and for grain sizes below 10 nm, grain boundary sliding is the dominant deformation mechanism [19]. By analyzing the behavior of crack tip plasticity on the change in the near-tip field quantities of the plastic zone in different NC alloys with different configurations of grain size distribution, it was possible to study the problem of a crack approaching the interfaces at which the plastic properties of the material change continuously and linearly [20]. It was observed that the J -integral decreases when passing from the harder to the softer material, demonstrating that the potential energy for crack propagation increases in the negative plastically graded configuration (in which the grain size linearly varies between 20 and 100 nm from the surface to the bottom), while the potential energy decreases in the case of positive graded configuration (in which the grain size linearly varies between 100 and 20 nm from the surface to the bottom). The J -integral variation in the negative and positive configurations, as compared with the constant 100 nm grain size for

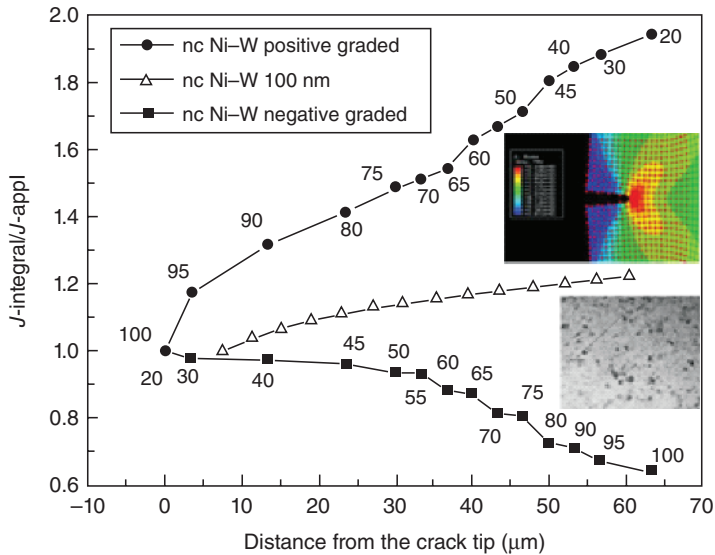


Figure 1.9 Comparison between the calculations of the J -integral for the negative and positive plastically graded sheets.

Ni–W electrodeposited alloy, is shown in Figure 1.9. From this study, it can be concluded that the graded properties of the electrodeposited alloys play a very important role in the control of crack growth, and particularly, the negative graded configuration appears very useful in reducing the crack growth rate.

From the engineering point of view, the aforementioned result is very useful; in fact, it is demonstrated that, for NC metals, the susceptibility to crack initiation decreases with decreasing grain size while it increases the crack propagation rate. By producing structures with negative graded configuration, it is possible to obtain a surface with very low susceptibility to crack initiation and a bulk structure in which the crack growth rate is continuously decreased in each section.

1.6

Conclusions

The analyses of the microstructural and mechanical properties of nanostructured materials lead to very bright horizons to new researches and industrial applications. This chapter describes the increase in the mechanical properties of nanostructured metals and alloys by increasing the grain refinement up to a level at which the grain size volume begins influencing the dislocation generation and motion, leading to an inversion in such a behavior, well known as *Hall–Petch inversion*. The microstructural and mechanical features of nanostructured materials strongly depend on the production techniques. Actually, UFG metals produced via SPD exhibit a refining limit of few hundreds of nanometers depending on the

total deformation strain. Such severe deformation leads to a microstructure characterized by a high dislocation energy level, which leads to a material very sensitive to room- and high-temperature deformation and to the microstructure modifications as a consequence of heat treatments. Grain refinement can be improved by employing different processing techniques such as electrodeposition. Such techniques can obtain pure bulk metals characterized by grain sizes below 10 nm without defects. A decrease in the grain size down to such levels has a strong effect on the increase in strength but coupled with a large reduction in ductility. Additionally, the hardening behavior is strongly influenced by the grain size at such refining levels. These aspects are well evidenced by employing a characterization technique such as instrumented nanoindentation, which is capable of probing nanostructured materials in a broad range of forces, strains, and strain rates. This technique was revealed to be very useful in measuring the strain rate sensitivity of nanostructured metals in a broad range of grain sizes, leading to the definition of deformation mechanisms during strain in NC metals and alloys. Very useful information is obtained from the study of fatigue properties of aforementioned class of new materials. UFG materials produced via SPD show an increase in fatigue limit with decreasing grain size in the high cycle regime; the low cycle behavior is strongly influenced by dislocation mechanisms such as large deformation recovery. For the materials produced via SPD, even if grain refinement leads to an increase in the number of cycles to failure at the same stress levels investigated, the results for very close microstructures (20 and 40 nm) resulted in a strong function of the ductility (very high stresses). In addition, by analyzing the strain amplitude as a function of the number of cycles to failure for all the electrodeposited materials, it can be concluded that the sensitivity to cyclic hardening increases by decreasing the material mean grain size. For such materials, produced via electrodeposition, the fatigue crack growth tests, performed over a broad range of stress levels, revealed that these materials are less sensitive to crack initiation with decreasing mean grain size while the resistance to crack growth decreases with grain refinement. A very interesting perspective is achieved by the possibility of producing plastically graded bulk structures via electrodeposition. By tuning the electrodeposition current and the bath temperature, it is possible to vary the material composition in terms of the alloying elements, consequently varying the grain size along with the thickness of the thin films. The analyses of fatigue properties of such structures showed the possibility to control the grain size initiation and growth through the control of grain size and distribution along the crack paths.

References

1. Gleiter, H. (2000) Nanostructured materials: basic concepts and microstructure. *Acta Mater.*, **48**, 1–29.
2. Meyers, M.A., Mishra, A., and Benson, D.J. (2006) Mechanical properties of nanocrystalline materials. *Prog. Mater. Sci.*, **51**, 427–556.
3. Cavaliere, P. (2008) Strain rate sensitivity of ultra-fine and nanocrystalline metals and alloys. *Physica B*, **403**, 569–575.

4. Valiev, R.Z., Islamgaliev, R.K., and Alexandrov, I.V. (2000) Bulk nanostructured materials from severe plastic deformation. *Prog. Mater. Sci.*, **45**, 103–189.
5. Valiev, R.Z. and Langdon, T.G. (2008) Using high-pressure torsion for metal processing: fundamentals and applications. *Prog. Mater. Sci.*, **53**, 893–979.
6. Zhu, Y.T. and Lowe, T.C. (2000) Observations and issues on mechanisms of grain refinement during ECAP process. *Mater. Sci. Eng. A*, **A291**, 46–53.
7. Zhilyaev, A.P., Kim, B.-K., Szpunar, J.A., Bar'o, M.D., and Langdon, T.G. (2005) The microstructural characteristics of ultrafine-grained nickel. *Mater. Sci. Eng. A*, **A391**, 377–389.
8. Cavaliere, P. (2009) Fatigue properties and crack behavior of ultra-fine and nanocrystalline pure metals. *Int. J. Fatigue*, **31**, 1476–1489.
9. Zhu, Y.T., Liao, X.Z., and Wu, X.L. (2012) Deformation twinning in nanocrystalline materials. *Prog. Mater. Sci.*, **57**, 1–62.
10. Valiev, R.Z. and Langdon, T.G. (2006) Principles of equal-channel angular pressing as a processing tool for grain refinement. *Prog. Mater. Sci.*, **51**, 881–981.
11. Sakaia, G., Horitaa, Z., and Langdon, T.G. (2005) Grain refinement and superplasticity in an aluminum alloy processed by high-pressure torsion. *Mater. Sci. Eng. A*, **A393**, 344–351.
12. Cavaliere, P. (2009) Mechanical properties of nanocrystalline metals and alloys studied via multi-step nanoindentation and finite element calculations. *Mater. Sci. Eng. A*, **A512**, 1–9.
13. Cavaliere, P. (2010) Cyclic deformation of ultra-fine and nanocrystalline metals through nanoindentation: similarities with crack propagation. *Procedia Eng.*, **2**, 213–222.
14. Wang, L., Gao, Y., Xu, T., and Xue, Q. (2006) A comparative study on the tribological behavior of nanocrystalline nickel and cobalt coatings correlated with grain size and phase structure. *Mater. Chem. Phys.*, **99**, 96–103.
15. Cavaliere, P. and Prete, P. (2010) Tribomechanisms of pure electrodeposited Ni at ultra-fine and nanoscale level. *Wear*, **268**, 1490–1503.
16. Mughrabi, H. and Höppel, H.W. (2010) Cyclic deformation and fatigue properties of very fine-grained metals and alloys. *Int. J. Fatigue*, **32**, 1413–1427.
17. Vinogradov, A. and Hashimoto, S. (2001) Multiscale phenomena in fatigue of ultra-fine grained materials-an overview. *Mater. Trans.*, **42** (1), 74–84.
18. Mughrabi, H., Höppel, H.W., and Kautz, M. (2004) Fatigue and microstructure of ultrafine-grained metals produced by severe plastic deformation. *Scr. Mater.*, **51**, 807–812.
19. Farkas, D., Willemann, M., and Hyde, B. (2005) Atomistic mechanisms of fatigue in nanocrystalline metals. *Phys. Rev. Lett.*, **94** (16), Art. No. 165502.
20. Cavaliere, P. (2008) Crack tip plasticity in plastically graded Ni–W electrodeposited nanocrystalline alloys. *Comput. Mater. Sci.*, **41**, 440–449.